ISSN 1330-3651 (Print), ISSN 1848-6339 (Online)
https://doi.org/10.17559/TV-20220804113958
Preliminary communication

Orthogonal Experiment Study on Mechanical Properties of Hybrid Fibre Reinforced Shale Ceramisite Concrete

Weijing YAO*, Mwenya MWENYA, Yushan LIU, Zhaolong YAO, Jianyong PANG

Abstract: The slump, cube compressive strength and splitting tensile strength tests of 9 groups of hybrid fiber reinforced shale ceramisite concrete (HFSC) and 1 group of C30 reference concrete were conducted by orthogonal experimental method. The effects of shale ceramisite volume replacement, basalt fiber volume fraction and polypropylene fiber volume fraction on the mechanical properties of HFSC were investigated. The results show that the splitting tensile strength and tension-compression ratio of concrete can be significantly improved by adding fiber, which plays a positive hybrid effect. The maximum increase in the tensile strength of concrete by basalt fiber and polypropylene fiber is 57.33% and 58.19% respectively, while the influence of compressive strength was small. Shale ceramisite significantly reduces the compressive and tensile strength of concrete. When the replacement increases from 0% to 15%, the compressive strength of HFSC decreases by 19.98%, while the tensile strength has underwent an iterative process of increasing and decreasing due to the fiber reinforcement effect. All three factors reduced the slump of concrete mixture. The shale ceramisite and basalt fiber have significant influence, and polypropylene fiber has a greater impact. The influence mechanism of three factors on mechanical properties of HFSC was revealed.The prediction models of cube compressive strength and splitting tensile strength of HFSC were obtained, and the accuracy of model is high.

Keywords: basalt fiber; mechanical properties; orthogonal experiment; polypropylene fiber; shale ceramisite concrete; strength prediction model

1 INTRODUCTION

Shale ceramsite, produced from the shale and ceramic ware waste, as coarse aggregate for structural concrete produced lightweight aggregate concrete, which has the characteristics of light weight, high strength, high durability, good frost resistance, heat insulation [1]. It can effectively reduce the weight of building structure and cross-sectional size. It is widely used in walls, buildings, bridge and road engineering. However, there are common defects in cement-based composite materials such as low tensile strength, flexural strength, and brittle failure. To make up for the above disadvantages, researchers have mixed fibers in concrete to prevent cracking, improve the toughness and brittleness [2].

Basalt fiber is an inorganic fiber made of pure natural volcanic eruption rock and rapidly drawn after melting at a high temperature of 1450 - 1500 ℃. It has some good characteristics of high elastic modulus, small thermal conductivity, large tensile strength, low price, easy dispersion and good compatibility in the cement matrix [3]. Polypropylene fiber is a bundle-like synthetic fiber, which has the advantages of light weight, easy dispersion, good toughening and cracks resistance, and less damage to the mixing machine [4]. These two new types of fibers overcome the shortcomings of steel fibers, such as large weight, easy rust, easy agglomeration, and damage to the mixing machine, which have received widespread attention recently. Studies have shown that the incorporation of multiple fibers to form hybrid fiber reinforced concrete (HFRC) can complement each other and exert positive hybrid effect [5], overcoming the limitation of single fiber on the performance of concrete. The current research on hybrid fiber concrete focuses on mixing high elastic modulus fibers (such as steel fiber, carbon fiber, basalt fiber) and high ductility fibers (such as polypropylene fiber, polyethylene fiber) to improve the comprehensive properties of the cement-based material. The current research on hybrid fiber mixed with shale ceramisite concrete has focused on steel-polypropylene fiber [6]. For example, Wang et al. used steel and polypropylene fibers to prepare plastic-steel hybrid fiber shale ceramisite concrete, which has good residual strength after multiple impact tests [7]. Libre and Badogiannis et al. also used steel and polypropylene fibers in contents of 0.5% and 1.0%, improving the ductility of pumice shale ceramisite concrete [8-9]. Huang et al. studied the mechanical properties of polypropylene and wood fibre reinforced expand polystyrene shale ceramisite concrete under various sand contents, and the damage constitutive model was proposed based on the tests results [10].

In this paper, shale ceramsite, basalt fiber and polypropylene fiber were used to prepare hybrid fiber reinforced shale ceramisite concrete (HFSC), which has some great characteristics of low cost, excellent mechanical properties, in line with the concept of environmental protection. The orthogonal test was designed and the influence of basalt fiber and polypropylene fiber on the mechanical properties of HFSC were investigated. There are three factors, including the shale ceramsite volume replacement, basalt fiber volume fraction and polypropylene fiber volume fraction, the tests of the slump of concrete mixture, cube compressive strength and splitting tensile strength of concrete specimen were completed.

2 MATERIALS AND METHODS

2.1 Raw Materials

Cement and fly ash were used as cementitious materials. The cement, used in this study, was made of Huainan Bagongshan P·C 42.5 composite Portland cement, China. Its main performance indicators are shown in Tab. 1. The fly ash was Grade I, produced by Huainan Pingwei Power Plant, China, the chemical composition is shown in Tab. 2. Coarse aggregate was calcareous crushed stone, continuous graded crushed stone with a particle size 5 - 15 mm, apparent density of 2650 kg/m^3. The fine aggregate was medium sand from Huaihe River, with a fineness modulus of 2.70, and apparent density of 2750 kg/m^3. Moreover, the water-reducing admixture was produced by Shanxi Qinfen Building Materials Factory,

with a water reduction rate of 28% and a mixing amount of 1% of the cementitious material.

Table 1 Performance of Bagongshan P·C 42.5 cement

Water requirement	SO_3 / %	MgO / %	Compressive strength / MPa		Lgnition loss / %
			3 d	28 d	
25.9	1.93	2.18	22.99	49.75	3.5

Table 2 Chemical composition of fly ash/%

SiO_2	Al_2O_3	Fe_2O_3	CaO	MgO	Na_2O	Lgnition loss
53.26	34.72	4.07	2.47	0.39	1.90	4.07

The test lightweight aggregate was shale ceramsite (SC) produced by Anhui Changcai Energy Conservation Company, Huainan, China. The physical performance indicators are shown in Tab. 3, and the photo is shown in Fig. 1a. Basalt fiber is chopped basalt fiber (BF) produced by a company in Jiangsu Proviance, China. The physical performance indicators are shown in Tab. 4. The photo is shown in Fig. 1b. The polypropylene fiber is a bundled monofilament polypropylene fiber (PF) produced by LangfangKaide Company, Langfang, China. The performance indexes are shown in Tab. 4, and the photos are shown in Fig. 1c.

Table 3 Performance indexes of shale ceramisite

Size / mm	Bulk density / kg/m^3	Apparent density / kg/m^3	Compressive strength / MPa	Water absorption / %
2 - 5	336	628	≥ 3.0	9.9

Table 4 Main performance parameters of basalt fiber and polypropylene fiber

Fiber	Diameter / μm	Length / mm	Density / g/cm^3	Elastic modulus / GPa	Tensile strength / MPa
Basalt fiber	5-20	3-25	2.65	90 - 110	3500 - 4500
Polypropylene fiber	18 - 48	12	0.91	≥ 2.5	≥ 300

(a) shale ceramisite (b) basalt fiber (c) polypropylene fiber

Figure 1 Raw materials of HFSC

2.2 Mix Ratio Design

The effects of fiber content and shale ceramsite content on mechanical properties of shale ceramisite concrete were considered by the orthogonal test method. The $L_9(3^3)$ orthogonal table was used to design the experiment, and the factors and levels were determined with reference to related research [3-9]. (1) The shale ceramsite volume replacement V_{SC} is 5%, 10%, and 15%, respectively of the total volume of coarse aggregate gravel stone; (2) The basalt fiber volume fraction V_{BF} in concrete is 0.2%, 0.3%, and 0.4%, respectively; (3) The polypropylene fiber volume fraction V_{PF} in concrete is 0.2%, 0.3%, and 0.4%, respectively. A total of 9 experimental groups and 1 reference group were designed, see Tab. 5 for details. S stands for reference concrete; HFSC stands for hybrid fiber reinforced shale ceramisite concrete.

Table 5 Proportion of test concrete (kg/m^3)

No.	V_{SC}	V_{BF}	V_{PF}	Cementing material		Stone	Sand	Water	Water reducer
				Cement	Fly ash				
S	0	0	0	450	50	1075	442	279	5.0
HFSC-1	54	5.28	1.80	450	50	1021	442	279	5.0
HFSC-2	54	7.92	2.70	450	50	1021	442	279	5.0
HFSC-3	54	10.56	3.60	450	50	1021	442	279	5.0
HFSC-4	108	5.28	2.70	450	50	967	442	279	5.0
HFSC-5	108	7.92	3.60	450	50	967	442	279	5.0
HFSC-6	108	10.56	1.80	450	50	967	442	279	5.0
HFSC-7	161	5.28	3.60	450	50	914	442	279	5.0
HFSC-8	161	7.92	1.80	450	50	914	442	279	5.0
HFSC-9	161	10.56	2.70	450	50	914	442	279	5.0

2.3 Experimental Design

Before test, to avoid twisting of the fibers, a preparation method of wet mixing and spreading the fibers performed simultaneously, was adopted. Besides, following Kong [11], the shale ceramsite was soaked in water for 1 hour, before preparation of concrete. First, the cement, calcareous gravel, sand and shale ceramsite were dry mixed for 1.5 minutes, then water and water reducing agent were added, and the basalt fiber and polypropylene fiber were sprinkled at the same time for wet stirring for 2.5 minutes.

The cube test specimen of 100 × 100 ×100 mm was used, and the molds were dismantled after 1 day of molding, and cured for 28 days under standard curing conditions with relative humidity ≥ 95% and temperature (20 ± 1℃), completing the concrete preparation. The cube compressive strength and splitting tensile strength tests were performed. The tension-compression ratio was calculated according to the test results. Finally, some samples were taken from the crushed test specimen, and the interfacial transition zone between fiber and cement matrix was microscope observed and analyzed. The completed concrete samples are shown in Fig. 2.

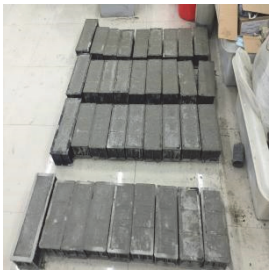

Figure 2 Concrete sample for mechanical property test

2.4 Test Method

The slump bucket was used to test the slump of concrete mix. The concrete mix was evenly loaded into the bucket three times, the height was about 1/3 of the bucket height, and each layer was vibrated for 25 times. After filling the slump bucket, the slump bucket was raised, and

the height difference between the bucket height and the highest point of the concrete mix was measured, which is the slump value.

The electro-hydraulic servo pressure testing machine was used for concrete strength. For compressive strength, the loading speed was 0.5 MPa/s, it is calculated according to Eq. (1).

$$f_{cu} = \frac{F}{A} \tag{1}$$

where, f_{cu} is the compressive strength of concrete, MPa; F is the failure load of the concrete specimen; A is the bearing area of concrete specimen, mm^2.

For tensile strength, the method of splitting strength test was adopted. The loading speed was 0.05 MPa/s, it is calculated according to Eq. (2).

$$f_{ts} = \frac{2F}{\pi A} \tag{2}$$

where, f_{ts} is the tensile strength of concrete, MPa; F is the failure load of the concrete specimen; A is the splitting surface area of concrete specimen, mm^2.

The tension-compression ratio was calculated according to the test results.

3 RESULTS AND ANALYSIS

3.1 Test Results

The test results are shown in Tab. 6. It can be seen that the slump and compressive strength of the hybrid fiber shale ceramisite concrete of all groups were reduced to different degrees compared to the reference concrete (S). HFSC-9 sample has the lowest slump and compressive strength, which are 79.19% and 22.51% lower than S sample, respectively. However, the splitting tensile strength has been significantly improved. The highest splitting strength of HFSC-3 sample is 71.55% higher than S sample. As a result, the tension-compression ratio is significantly increased, with HFSC-6 has the largest tension-compression ratio, which is 89.55% higher than S sample.

Table 6 Test results of HFSC

No.	Factor			Slump / mm	f_{cu} / MPa	f_{ts} / MPa	f_{ts}/f_{cu}
	A / %	B / %	C / %				
S	0	0	0	173	32.79	2.32	0.0708
HFSC-1	5	0.2	0.2	108	32.68	3.61	0.1105
HFSC-2	5	0.3	0.3	84	30.63	3.80	0.1241
HFSC-3	5	0.4	0.4	68	30.30	3.98	0.1315
HFSC-4	10	0.2	0.3	76	28.06	3.40	0.1212
HFSC-5	10	0.3	0.4	61	26.27	3.75	0.1427
HFSC-6	10	0.4	0.2	59	27.23	3.65	0.1342
HFSC-7	15	0.2	0.4	56	26.16	3.27	0.1250
HFSC-8	15	0.3	0.3	55	27.14	3.25	0.1197
HFSC-9	15	0.4	0.2	36	25.41	3.32	0.1306

The influence of three factors on the mechanical performances of the HFSC concrete was investigated, and the significant influencing factors were found out. The statistical analysis software Minitab was used to perform the analysis of range and variance. The results are shown in Tab. 7 and Tab. 8. According to Tab. 7, the trend of each performance at different levels of each factor is visualized in Fig. 3.

Table 7 Range analysis of HFSC

Index	Range	Shale ceramisite (A)	Basalt fiber (B)	Polypropylene fiber (C)
Slump / mm	k_1	86.67	80.00	74.00
	k_2	65.33	66.67	65.33
	k_3	49.00	54.33	61.67
	R	37.67	25.67	12.33
	Order	A > B > C		
f_{cu} / MPa	k_1	31.20	28.97	29.02
	k_2	27.19	28.01	28.03
	k_3	26.24	27.65	27.58
	R	4.96	1.32	1.44
	Order	A > C > B		
f_{ts} / MPa	k_1	3.80	3.43	3.50
	k_2	2.60	3.60	3.51
	k_3	3.28	3.65	3.67
	R	0.52	0.22	0.16
	Order	A > B > C		
f_{ts}/f_{cu}	k_1	0.1220	0.1189	0.1215
	k_2	0.1327	0.1288	0.1253
	k_3	0.1251	0.1321	0.1331
	R	0.0107	0.0132	0.0116
	Order	B > C > A		

Table 8 Variance analysis of HFSC

Index	Factor	Sum of square	Freedom	Mean square	F value	significance
Slump / mm	Shale ceramisite (A)	2140.67	2	1070.33	267.58	**
	Basalt fiber (B)	988.67	2	494.33	123.58	**
	Polypropylene fiber (C)	240.67	2	120.33	30.08	*
	Error	8.00	2	4.00		
f_{cu} / MPa	Shale ceramisite (A)	41.7039	2	20.8519	104.10	**
	Basalt fiber (B)	2.7857	2	1.3928	6.95	-
	Polypropylene fiber (C)	3.2491	2	1.6245	8.11	-
	Error	0.4006	2	0.2003		
f_{ts} / MPa	Shale ceramisite (A)	0.4080	2	0.2040	301.00	**
	Basalt fiber (B)	0.0824	2	0.0412	60.80	*
	Polypropylene fiber (C)	0.0523	2	0.0261	38.57	*
	Error	0.0014	2	0.0007		
f_{ts}/f_{cu}	Shale ceramisite (A)	1.81×10^{-4}	2	0.90×10^{-4}	6.54	-
	Basalt fiber (B)	2.84×10^{-4}	2	1.42×10^{-4}	10.25	(*)
	Polypropylene fiber (C)	2.10×10^{-4}	2	1.05×10^{-4}	7.57	-
	Error	0.28×10^{-4}	2	0.14×10^{-4}		

Note: $F_{0.01}(2, 2) = 99.0$, $F_{0.05}(2, 2) = 19.0$, $F_{0.1}(2, 2) = 9.0$. If $F > F_{0.01}(2, 2)$, which represents the factor has a significant influence, denoted with **; If $F_{0.05}(2, 2) < F < F_{0.01}(2, 2)$, indicating that the factor has a greater impact, denoted with *. If $F_{0.1}(2, 2) < F < F_{0.05}(2, 2)$, indicating that the factor has an impact, denoted with (*). If $F < F_{0.1}(2, 2)$, which means that the factor is almost of no influence.

3.2 The Slump of Concrete Mixture

From Tab. 7, for the influence of various factors on the slump of concrete mixture, the effect of shale ceramsite volume replacement was the largest, with a range of 37.67 mm, followed by the basalt fiber volume fraction, with a range of 25.67 mm, followed by the polypropylene

volume fraction, with a range of 12.33 mm. According to Tab. 8, the shale ceramsite volume replacement (A) and basalt fiber volume fraction (B) have significant influence on slump of fresh concrete mixture, and polypropylene fiber volume fraction (C) has a greater impact.

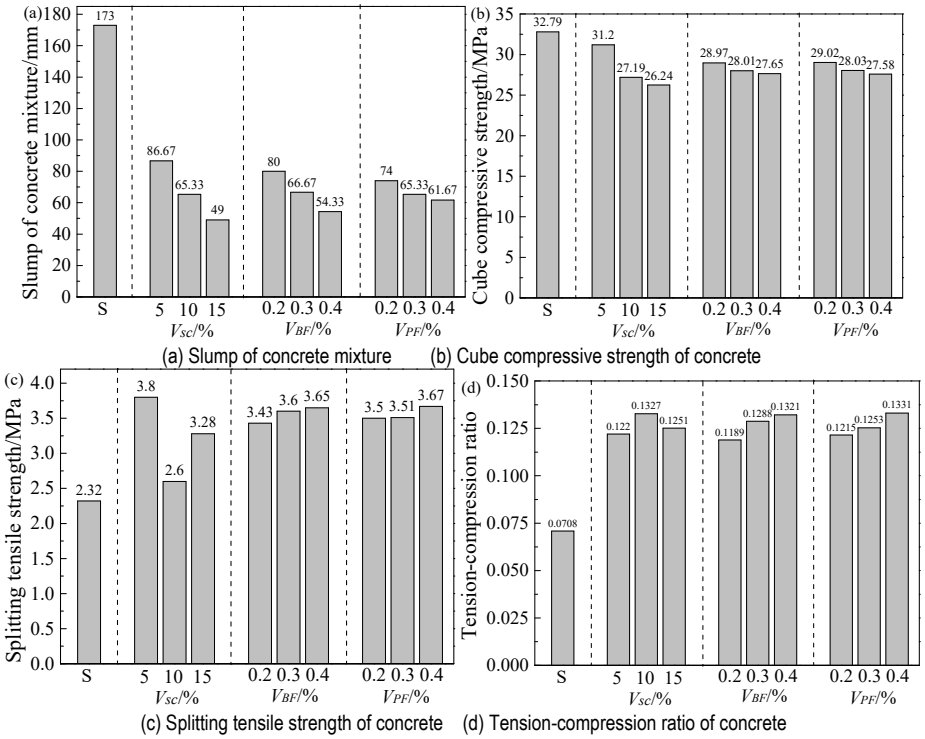

Figure 3 The properties of HFSC under various factors and levels

According to Fig. 3a, the slump of the concrete mixture gradually decreased with the increase of shale ceramsite volume replacement V_{SC}, basalt fiber volume fraction V_{BF} and polypropylene fiber volume fraction V_{PF}. Compared with the reference concrete (S), the slump of the HFSC mixture has decreased significantly, and the decline exceeded by 50%. The V_{SC} increased from 5% to 15% and slump decreased by 43.46%. The V_{BF} increased from 0.2% to 0.4% and slump decreased by 32.09%. The V_{PF} increased from 0.2% to 0.4% and slump decreased by 16.66%.

3.3 Cube Compressive Strength

From Tab. 7, the volume replacement of shale ceramsite has the largest influence on the cube compressive strength of HFSC, with a range of 4.96 MPa; the degree of influence of polypropylene fiber volume fraction was the second, with a range of 1.44 MPa; the degree of influence of basalt fiber volume fraction was the smallest, with a range of 1.32 MPa. According to Tab. 8, the shale ceramsite volume replacement has a significant influence on compressive strength of concrete, and the basalt fiber volume fraction and polypropylene fiber volume fraction have almost no influence on compressive strength of concrete.

According to Fig. 3b, compared with the reference concrete, the incorporation of ceramsite lightweight aggregate and fibers has a weakening of the compressive strength of the concrete, with different degrees. The V_{SC} increased from 5% to 10% and compressive strength decreased by 12.85%, the V_{SC} increased from 10% to 15% and compressive strength decreased by 3.49%. The V_{BF} increased from 0.2% to 0.3% and compressive strength decreased by 3.31%, the V_{BF} increased from 0.3% to 0.4% and compressive strength decreased by 1.29%. The V_{PF} increased from 0.2% to 0.3% and compressive strength decreased by 3.41%, the V_{PF} increased from 0.3% to 0.4% and compressive strength decreased by 1.61%.

It can be seen that the incorporation of shale ceramsite has a significant weakening influence on the compressive strength of concrete, while the fiber has a weakening influence on the compressive strength, but the influence is small. Besides, polypropylene fiber and basalt fiber, as low elastic modulus, exert a good tensile effect when cracks appear on the specimen. However, in the compressive test, the confined area of concrete specimen was reduced, so the compressive strength has a small weakening effect.

3.4 Splitting Tensile Strength

Based on Tab. 7, the shale ceramsite volume replacement has the largest influence on the splitting tensile strength of HFSC, with a range of 0.52 MPa, followed by the basalt fiber volume fraction, with a range of 0.22 MPa. The polypropylene fiber volume fraction has the smallest influence, with a range of 0.16 MPa. According to Tab. 8, the shale ceramsite volume replacement has a significant influence on tensile strength, and the basalt fiber volume fraction and polypropylene fiber volume fraction have a greater impact on tensile strength, and the influence degrees of the two fibers are close.

According to Fig. 3c, the V_{SC} increased from 5% to 10%, splitting tensile strength decreased by 31.58%, while the V_{SC} increased from 10% to 15%, splitting tensile

strength increased by 26.15%. The V_{BF} increased from 0.2% to 0.3% and splitting tensile strength increased by 4.96%, the V_{BF} increased from 0.3% to 0.4% and splitting tensile strength increased by 1.39%. The V_{PF} increased from 0.2% to 0.3% and splitting tensile strength increased by 0.29%, the V_{PF} increased from 0.3% to 0.4% and splitting tensile increased by 4.56%. It can be seen that shale ceramsite has a significant weakening influence on the tensile strength of concrete, and fiber incorporation can significantly increase the tensile strength, and the influences of the two fibers are relatively close.

3.5 Tension-Compression Ratio

Based on Tab. 7, the basalt fiber volume fraction has the largest influence on the tension-compression ratio of HFSC, with a range of 0.0132, followed by the polypropylene fiber volume fraction, with a range of 0.0116. The shale ceramsite volume replacement has the smallest influence, with a range of 0.0107. According to Tab. 8, it can be obtained that only the basalt fiber volume fraction has an impact on the tension-compression ratio, and shale ceramsite volume replacement and polypropylene fiber volume fraction have almost no influence on tension-compression ratio. However, the contribution of polypropylene fiber volume fraction to the tension-compression ratio is greater than the contribution of shale ceramsite volume replacement.

According to the Fig. 3d, the V_{SC} increased from 5% to 10% and the tension-compression ratio increased by 8.77%, while the V_{SC} increased from 10% to 15% and the tension-compression ratio decreased by 5.73%. The V_{BF} increased from 0.2% to 0.3% and tension-compression ratio increased by 8.33%, the V_{BF} increased from 0.3% to 0.4% and tension-compression ratio increased by 2.56%. The V_{PF} increased from 0.2% to 0.3% and tension-compression ratio increased by 3.13%, the V_{PF} increased from 0.3% to 0.4% and tension-compression ratio increased by 6.23%. It can be seen that the incorporation of fibers effectively improves the tensile strength and also improves the tension-compression ratio.

3.6 Analysis of Factors Influencing HFSC Performance

3.6.1 The Influence of Shale Ceramsite

Shale ceramsite is the most common lightweight coarse aggregate in China. Its micro-morphology is shown in Fig. 4. From the figure, the interior is a porous foam structure with a large pore size, which partially closes the spherical pores, and the pores connected to the passage, showing a clear network structure. The outer surface has a dense surface layer with a thickness of less than 1 mm, which has a coarse ceramic structure with a pore diameter much smaller than the pore diameter of the internal foam structure [12].

The above structure determines that shale ceramsite has good characteristics of light weight, water absorption, produces self-curing effect in cement-based materials, and overcomes the disadvantage of weak interface zone between aggregate and cement matrix [13]. Fig. 5 shows the interfacial transition zone micro-structures of shale ceramisite, stone and cement matrix. From the Fig. 5a, the ceramsite continuously releases water in the curing process, and the cement at the inerfacial transition zone becomes more dense. From Fig. 5b, the fracture at the interface between stone and cement matrix is the internal cause of concrete failure. However, the strength of shale ceramsite is relatively low, compared to the normal calcareous gravel, and material damage often occurs along with the shale ceramsite aggregate. Porous water absorption also resulted in a decreasing in the fluidity and slump of the concrete mixture. Besides, the continuous gradation of calcareous pebbles with a more uniform particle size of shale ceramsite also affected the workability of the concrete mixture.

3.6.2 The Influence of Basalt Fiber

The basalt fibers were mixed into the concrete to form a non-directional support system, which prevented the separation of the various components of the concrete, thereby greatly reducing the fluidity of concrete mixture. The hardened fiber-reinforced composite material was first borne by concrete matrix when under loading. As concrete micro-cracks were generated and gradually expanded, basalt fibers with high elastic modulus played a reinforcing role through the bonding force and mechanical occlusion force with the cement matrix. However, the strengthening effect was better reflected in the increasing of tensile strength while decreasing of compressive strength. This is because the fiber does not disperse well in the cement matrix, which reduces the compactness of the concrete and reduces the effective bearing area of the concrete.

From the micro-morphology of the basalt fiber pulled out of the cement matrix in Fig. 6. Based on the figure, there are more cement hydration products attached to the basalt fiber surface, and the basalt fiber and the cement matrix are tightly bound, which play a role in preventing the development of cracks, reinforcing and anchoring during the stress loading.

3.6.3 The Influence of Polypropylene

For polypropylene fiber, as the concrete cracks further expand, the bonding force and occlusal force between the basalt fiber and the matrix decrease. However, the crack growth-inhibiting force of polypropylene fiber is reflected, as high ductility and low elastic modulus fiber. The fibers transmit the stress to the un-cracked concrete hardened body. When the stress of the adjacent hardened body reached the ultimate tensile strength, new micro-cracks were generated, which produced a multi-fracture effect, which made the internal stress of the structure tend to be uniformly distributed. Besides, since the deformation was mostly elastic, polypropylene fibers can absorb energy in the form of elastic deformation energy under repeated loading [14]. As a result, polypropylene fiber mixed with basalt fiber, showing positive mixing effect.

It can be seen from the scanning electron microscope after the polypropylene fiber was pulled out in Fig. 7. It shows that after the failure of the concrete specimen, the polypropylene fiber still plays a role of bridging the cement matrix, which improves the ductility, toughness and post-fracture properties of the concrete.

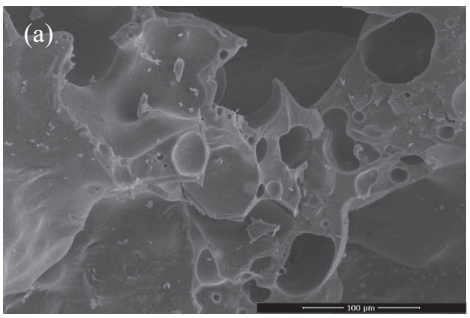

(a) Core

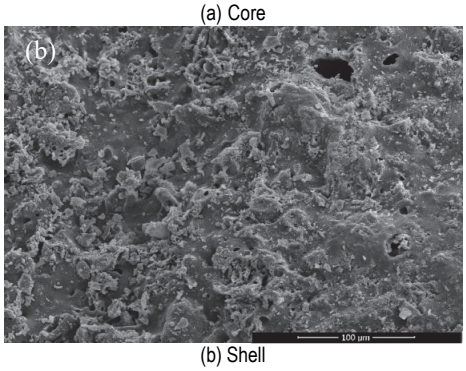

(b) Shell

Figure 4 Microstructure of shale ceramisite

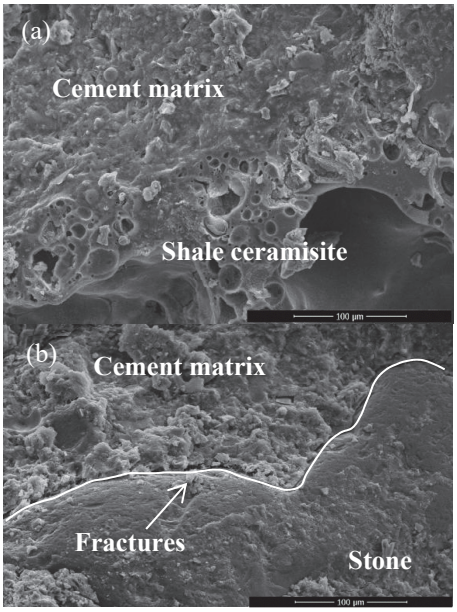

Figure 5 Interfacial transition zone micro-structures of shale ceramisite, stone and cement matrix

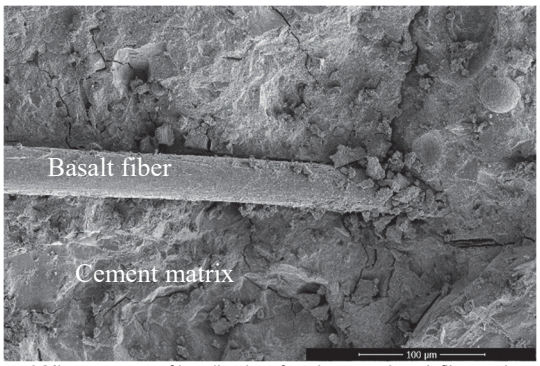

Figure 6 Microstructure of bonding interface between basalt fiber and cement matrix

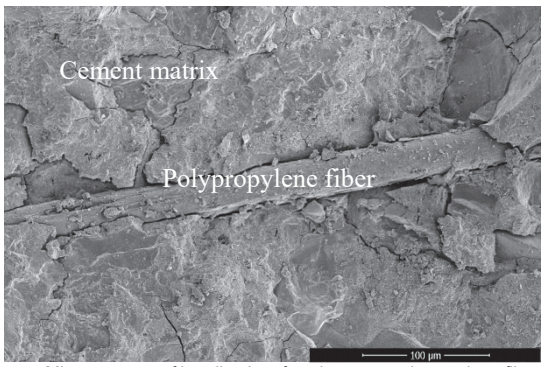

Figure 7 Microstructure of bonding interface between polypropylene fiber and cement matrix

4 STRENGTH PREDICTION MODEL

According to the theory of composite material mechanics, it is assumed that the strength of this concrete has four parts, included the strength of reference concrete, influence item of shale ceramsite volume replacement, influence item of basalt fiber volume fraction, and influence item of polypropylene fiber volume fraction, which can form a strength prediction model of HFSC. The strength regression model is:

$$f = f_0 + \alpha_1 x_1 + \alpha_2 x_2 + \alpha_3 x_3 \tag{3}$$

where f is the cube compressive strength or splitting tensile strength of concrete (MPa); f_0 is the cube compressive strength or splitting tensile strength of the reference concrete (MPa); α_1, α_2, α_3 are regression coefficients; x_1 is the shale ceramsite volume replacement (%); x_2 is the basalt fiber volume fraction (%); x_3 is the polypropylene fiber volume fraction (%).

The data in Tab. 6 is substituted into the regression model Eq. (3), regression fitting calculation was performed for each coefficient, and the regression formulas were obtained for compressive strength and tensile strength of HFSC. The fitting formulas were obtained as follows.

$$\begin{aligned} f_{cu} &= 37.3156 - 49.67x_1 - 660.00x_2 - 720.00x_3 \\ R^2 &= 0.82 \end{aligned} \tag{4}$$

$$\begin{aligned} f_{ts} &= 3.4956 - 5.17x_1 + 111.67x_2 + 81.67x_3 \\ R^2 &= 0.92 \end{aligned} \tag{5}$$

where, f_{cu} is cube compressive strength of concrete (MPa); $f_{ts}$is splitting strength of concrete (MPa); R^2 is relative coefficient.

The model predicted values and experimentally measured values of cube compressive strength and splitting tensile strength of HFSC are shown in Fig. 8. From the Table, the maximum errors of compressive strength and tensile strength all appear in HFSC-5, with error values of 4.64% and −2.93%, respectively, which indicates that the model has better accuracy.

In view of the large differences in the physical properties and mix ratio design of shale ceramsite lightweight aggregates, reference to the literature similar to the test conditions in this paper, the comparisons between the calculated value of HFSC cube compressive and

splitting strength prediction model in this study and the test results in the literature [15-19], are shown in Tab. 9.

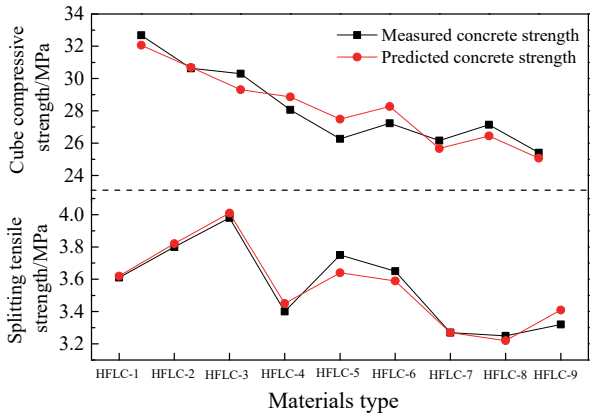

Figure 8 Comparison of predicted values with measured values of strength of HFSC

In Tab. 9, the serial numbers 1 - 12 are the data in the literature [15], reference concrete f_{cu} = 39.2 MPa, 32.5 Portland slag cement, water-cement ratio 0.5 were used. The serial numbers 13 - 20 are the data in the literature [16], reference concrete f_{cu} = 34.0 MPa, f_{ts} = 2.83 MPa, 32.5 Portland slag cement, water-cement ratio 0.5 were used. The serial numbers 21 - 25 are the data in the literature [17], reference concrete f_{cu} = 40.5 MPa, f_{ts} = 3.64 MPa, 42.5 ordinary Portland cement, water-binder ratio 0.6 were used. The serial numbers 26 - 29 are the data in the literature [18], reference concrete f_{cu} = 32.4 MPa, f_{ts} = 2.83 MPa, 42.5 ordinary Portland cement, water-cement ratio 0.45, and fly ash ceramsite as lightweight aggregate were used. The serial numbers 30 - 31 are the data in the literature [19], reference concrete f_{cu} = 33.21 MPa, f_{ts} = 2.92 MPa, water-cement ratio 0.43, and shale ceramsite as lightweight aggregate were used. Based on Tab. 9, the prediction model established in this paper can well verify the experimental results of other scholars, and the maximum error is mostly about 10%.

Table 9 Comparison of strength prediction model with other research results [15-19]

Literature	Number	V_{BF} / %	V_{PF} / %	f_{cu} / MPa		Relative error / %	f_{ts} / MPa		Relative error / %
				Test	Calculated		Test	Calculated	
Literature [15]	1	0.15	0.15	33.0	35.25	6.80	-	-	-
	2	0.30	0.30	31.9	33.18	4.00	-	-	-
	3	0.45	0.45	30.5	31.11	1.99	-	-	-
	4	0.60	0.60	32.9	29.04	-11.75	-	-	-
	5	0.10	0.20	38.8	35.22	-9.24	-	-	-
	6	0.20	0.40	35.8	33.12	-7.50	-	-	-
	7	0.30	0.60	28.0	31.02	10.77	-	-	-
	8	0.40	0.80	28.6	28.92	1.10	-	-	-
	9	0.20	0.10	38.0	35.28	-7.17	-	-	-
	10	0.40	0.20	35.1	33.24	-5.31	-	-	-
	11	0.60	0.30	29.0	31.20	7.57	-	-	-
	12	0.80	0.40	27.1	29.16	7.59	-	-	-
Literature [16]	13	0.06	0	34.5	36.92	7.01	3.14	3.56	13.46
	14	0.12	0	33.3	36.52	9.68	3.16	3.63	14.86
	15	0	0.06	37.5	36.88	−1.64	3.18	3.54	11.47
	16	0.06	0.06	38.3	36.49	−4.73	3.58	3.61	0.88
	17	0.12	0.06	38.2	36.09	−5.52	3.62	3.68	1.62
	18	0	0.12	36.1	36.45	0.97	2.89	3.59	24.35
	19	0.06	0.12	37.9	36.06	−4.87	3.31	3.66	10.59
	20	0.12	0.12	37.0	35.66	−3.62	3.34	3.73	11.61
Literature [17]	21	0.05	0	39.3	36.99	−5.89	3.70	3.55	−4.02
	22	0.1	0	26.9	36.66	36.27	3.02	3.61	19.45
	23	0.2	0	28.3	36.00	27.19	3.19	3.72	16.58
	24	0	0.1	40.6	36.60	−9.86	4.25	3.58	−15.83
	25	0.1	0.1	40.9	35.94	−12.14	3.96	3.69	−6.84
Literature [18]	26	0.05	0	32.7	36.99	13.11	2.95	3.55	20.39
	27	0.1	0	33.2	36.66	10.41	3.13	3.61	15.25
	28	0.15	0	33.7	36.33	7.79	3.28	3.66	11.68
	29	0.2	0	33.1	36.00	8.75	3.16	3.72	17.69
Literature [19]	30	0	0.05	33.3	36.96	10.98	3.29	3.54	7.49
	31	0	0.1	37.4	36.60	−2.15	3.30	3.58	8.40

5 CONCLUSION

(1) The shale ceramsite volume replacement, basalt fiber volume fraction, and polypropylene fiber volume fraction all resulted in a significant reduction in the slump of the concrete mixture. The shale ceramsite volume replacement and basalt fiber volume fraction are significant factors influencing the slump of fresh concrete mixture, and polypropylene fiber volume fraction has a greater impact.

(2) Basalt fiber and polypropylene fiber have a significant enhancement effect on the tensile strength of HFSC. When the volume fraction of basalt fiber (V_{BF}) and polypropylene fiber (V_{PF}) increased from 0% to 0.4%, the tensile strength of HFSC increased by 57.33% and 58.19%, respectively. The effect of the two fibers on the improvement of tensile strength is close while the shale ceramsite volume replacement (V_{SC}) has a greater weakening effect on the tensile strength. The influence of various factors on the concrete tensile strength is as follows: shale ceramsite volume replacement (V_{SC}) > basalt fiber volume fraction (V_{BF}) > polypropylene fiber volume fraction (V_{PF}).

(3) The shale ceramsite volume replacement (V_{SC}) has a significant weakening effect on the cube compressive strength of concrete. When the shale ceramsite volume

replacement (V_{SC}) increased from 0% to 15%, the cube compressive strength of HFSC decreased by 19.98%, while the volume fraction of basalt fiber (V_{BF}) and polypropylene fiber (V_{PF}) has almost no influence on cube compressive strength.

(4) Due to the positive hybrid effects of two fibers with different elasticity modulus, the stiffening, anchoring, and multi-fracture effects were effectively formed in the initial, development and failure stages of the concrete specimen. As a result, the tension-compression ratio of HFSC was improved. The degree of each influence factor is as follows: basalt fiber volume fraction (V_{BF}) > polypropylene fiber volume fraction (V_{PF}) > shale ceramsite volume replacement (V_{SC}).

(5) Based on the test results, a prediction model of cube compressive strength and splitting tensile strength of HFSC was established. Compared with experimental data of related works of literature, the verification showed that the prediction model has a high accuracy, which can be the reference for engineering application.

Acknowledgements

The authors acknowledge School of Civil Engineering and Architecture, Anhui University of Science and Technology for their support to perform this research. This work was also supported by Key Project of Natural Science Research in Colleges and Universities in Anhui Province, China (KJ2020A0297), the Science and Technology Project of Huainan City, Anhui Province, China (2021022).

6 REFERENCES

[1] Julia, G. G., Desirée, R. R., Andrés, J. V., Julia, M. M. P., & M. Ignacio, G. R. (2015). Ceramic ware waste as coarse aggregate for structural concrete production. *Environment Technology*, *36*(23), 3050-3059. https://doi.org/10.1080/09593330.2014.951076

[2] Md, A. O. M., Mohd, N. M. N., & Anas, A. S. (2022). Mechanical properties of low densities lightweight foamed concrete strengthen with raw empty fruit bunch fibre. *Tehnicki Vjesnik-Technical Gazette*, *29*(2), 646-651. https://doi.org/10.17559/TV-20210413123325

[3] Jiang, C. H., Fan, K., & Wu, F. (2014). Experimental study on the mechanical properties and microstructure of chopped basalt fibre reinforced concrete. *Materials and Design*, *58*, 187-193. https://doi.org/10.1016/j.matdes.2014.01.056

[4] Lee, J. H., Cho, B., & Choi, E. (2016). Experimental study of the reinforcement effect of macro-type high strength polypropylene on the flexural capacity of concrete. *Construction and Building Materials*, *126*, 967-975. https://doi.org/10.1016/j.conbuildmat.2016.09.017

[5] Quan, C. Q., Jiao, C. J., & Yang, Y. Y. (2019). Orthogonal experimental study on mechanical properties of hybrid fiber reinforced concrete. *Journal of Building Materials*, *22*(3), 363-370.

[6] Hassanpour, M., Shafigh, P., & Mahmud, H. B. (2012). Lightweight aggregate concrete fiber reinforced. *Construction and Building Materials*, *37*, 452-461. https://doi.org/10.1016/j.conbuildmat.2012.07.071

[7] Wang, D., Guo, Z. K., Shao, F., & Cheng W. X. (2014). Dynamic mechanical properties of plastic steel hybrid fibers reinforced lightweight aggregate concrete. *Journal of the Chinese Ceramic Society*, *42*(10), 1253-1259.

[8] Libre, N. A., Shekarchi, M., Mahoutian, M., & Soroushian, P. (2011). Mechanical properties of hybrid fiber reinforced lightweight aggregate concrete made with natural pumice. *Construction and Building Materials*, *25*, 2458-2464. https://doi.org/10.1016/j.conbuildmat.2010.11.058

[9] Badogiannis, E. G., Christidis, K. I., & Tzanetatos, G. E. (2019). Evaluation of the mechanical behavior of pumice lightweight concrete reinforced with steel and polypropylene fibers. *Construction and Building Materials*, *196*, 443-456. https://doi.org/10.1016/j.conbuildmat.2018.11.109

[10] Huang, W., Miao, X. W, Sun, Y. J, & Reng, S. S. (2020). Study on the mechanical properties and damage constitutive model of hybrid fibre-reinforced EPS lightweight aggregate concrete. *Tehnicki Vjesnik-Technical Gazette*, *27*(6), 1836-1843. https://doi.org/10.17559/TV-20190428142148

[11] Kong, L. J. & Du, Y. B. (2015). Effect of lightweight aggregate and the interfacial transition zone on the durability of concrete based on grey correlation. *Indian Journal of Engineering and Materials Science*, *22*(1), 111-119.

[12] Li, P. J. & Liu, X. B. (2004). Fundamental mechanical properties of concrete with high strength expanded shale. *Journal of Building Materials*, *7*(1), 113-116.

[13] Vaclavik, V., Dvorsky, T., Dirner, V., Daxner, J., & St'astny, M. (2012). Polyurethane foam as aggregate for thermal insulating mortars and lightweight concrete. *Tehnicki Vjesnik-Technical Gazette*, *19*(3), 665-672.

[14] Zhang, L. F., Yin, Y. L., Liu, J. W., & Liang, Q. S. (2014). Mechanical properties study on basalt fiber reinforced concrete. *Bulletin of the Chinese Ceramic Society*, *33*(11), 2834-2837.

[15] Zhao, B. B., He, J. J., Wang, X. Z., & Zheng, S. W. (2015). Experimental on frost resistance of basalt-polypropylene hybrid fiber reinforced concrete. *Journal of Liaoning Technical University (Natural Science)*, *34*(12), 1402-1407.

[16] He, J. J., Shi, J. P., Wang, X. Z., & Han, T. L. (2016). Effect of hybrid effect on the mechanical properties of hybrid fiber reinforced concrete. *Fiber Reinforced Plastics/Composites*, (9), 26-32.

[17] Zhang, P. H., Fang, S. G., & Hong, H. S. (2019). Comparative tests of mechanical properties and failure mechanism of different fiber-reinforced concrete. *Fiber Reinforced Plastics/Composites*, (6), 73-79.

[18] Li, J. J., Niu, J. G., Wu, Y. C., & Zhu, C. (2016). Experimental study on mechanical properties of chopped basalt fiber reinforced lightweight aggregate concrete. *Building Structure*, *46*(15), 47-51.

[19] Liu, S. B., Jin, Z. X., & Yao, P. F. (2018). Mechanical and frost resistance properties of lightweight aggregate concrete reinforced by hybrid fiber. *Journal of Wuhan Institute of Technology*, *40*(4), 435-439.

Contact information:

Weijing YAO, associate professor, PhD, master supervisor
(Corresponding author)
School of Civil Engineering and Architecture,
Anhui University of Science and Technology,
232001 Huainan, China
Engineering Research Center of Underground Mine Construction, Ministry of Education,
Anhui University of Science and Technology,
232001 Huainan, China
E-mail: yaoweijing0713@163.com

Mwenya MWENYA, master degree candidate
School of Civil Engineering and Architecture,
Anhui University of Science and Technology,
232001 Huainan, China
E-mail: mwenyamwenya9@gmail.com

Yushan LIU, lecture, PhD
School of Civil Engineering and Architecture,
Anhui University of Science and Technology,
232001 Huainan, China
E-mail: liuyushan1997@126.com

Zhaolong YAO, master
School of Civil Engineering and Architecture,
Anhui University of Science and Technology,
232001 Huainan, China
E-mail: 941010593@qq.com

Jianyong PANG, professor, PhD, doctoral supervisor
School of Civil Engineering and Architecture,
Anhui University of Science and Technology,
232001 Huainan, China
E-mail: pangjyong@163.com